© 2019. Published by The Company of Biologists Ltd | Journal of Experimental Biology (2019) 222, jeb195982. doi:10.1242/jeb.195982

RESEARCH ARTICLE

Resolving coral photoacclimation dynamics through coupled photophysiological and metabolomic profiling

Kathryn E. Lohr[1,*], Emma F. Camp[2], Unnikrishnan Kuzhiumparambil[2], Adrian Lutz[3], William Leggat[4], Joshua T. Patterson[1,5] and David J. Suggett[2]

ABSTRACT

Corals continuously adjust to short-term variation in light availability on shallow reefs. Long-term light alterations can also occur as a result of natural and anthropogenic stressors, as well as management interventions such as coral transplantation. Although short-term photophysiological responses are relatively well understood in corals, little information is available regarding photoacclimation dynamics over weeks of altered light availability. We coupled photophysiology and metabolomic profiling to explore changes that accompany longer-term photoacclimation in a key Great Barrier Reef coral species, *Acropora muricata*. High light (HL)- and low light (LL)-acclimated corals were collected from the reef and reciprocally exposed to high and low light *ex situ*. Rapid light curves using pulse-amplitude modulation (PAM) fluorometry revealed photophysiological acclimation of LL corals to HL and HL corals to LL within 21 days. A subset of colonies sampled at 7 and 21 days for untargeted LC-MS and GC-MS metabolomic profiling revealed metabolic reorganization before acclimation was detected using PAM fluorometry. Metabolomic shifts were more pronounced for LL to HL corals than for their HL to LL counterparts. Compounds driving metabolomic separation between HL-exposed and LL control colonies included amino acids, organic acids, fatty acids and sterols. Reduced glycerol and campesterol suggest decreased translocation of photosynthetic products from symbiont to host in LL to HL corals, with concurrent increases in fatty acid abundance indicating reliance on stored lipids for energy. We discuss how these data provide novel insight into environmental regulation of metabolism and implications for management strategies that drive rapid changes in light availability.

KEY WORDS: Coral reef, Light acclimation, Great Barrier Reef, Metabolite, Photosynthesis

INTRODUCTION

Light availability fundamentally regulates the ecological success of reef-building corals over space and time (Muir et al., 2015). However, corals within shallow reef habitats are exposed to light intensities that continually change over both transient (seconds to hours) and longer-term (days to weeks) time scales (Anthony et al., 2004). Consequently, corals have evolved many mechanisms to photo-protect or photo-enhance in order to optimize physiological performance of their algal endosymbionts (see Roth, 2014). Such mechanisms include physiological, morphological and behavioral adaptations of the coral host (e.g. Muscatine et al., 1984; Porter et al., 1984; Gates and Edmunds, 1999; Enríquez et al., 2005; Lesser et al., 2010) needed to fine-tune light exposure to the algal endosymbionts, as well as continual photophysiological adjustments of the algal endosymbionts themselves (e.g. Iglesias-Prieto et al., 2004; Frade et al., 2008).

Given the importance of light for sustaining coral productivity, it is unsurprising that many studies have investigated the ability of corals to acclimate to changes in light intensity, i.e. photoacclimation (e.g. Titlyanov et al., 2001; Anthony and Hoegh-Guldberg, 2003a; Hennige et al., 2008). Most of these studies to date have predominantly focused on 'steady-state' properties of photoacclimation (reviewed in Warner and Suggett, 2016), via photophysiological measurements from corals acclimated to long-term exposure to different light intensities that occur naturally (Anthony and Hoegh-Guldberg, 2003b; Frade et al., 2008; Winters et al., 2009; Hennige et al., 2010) or are imposed experimentally (Hennige et al., 2008; Schutter et al., 2011; Jeans et al., 2013; Langlois and Hoogenboom, 2014; Cohen and Dubinsky, 2015). However, repeated photophysiological measurements during photoacclimation are needed to provide insight on the fine-scale physiological changes that occur following dynamic alterations in light availability. Comparatively few studies have actually analyzed fine-scale time-dependent changes to coral photophysiology that capture the dynamics inherent to photoacclimation rate and extent. An earlier study (Anthony and Hoegh-Guldberg, 2003a) used repeated respirometry measurements to model changes in photophysiological parameters of *Turbinaria mesenterina* during acclimation to both increases and decreases in light. Actual photophysiological changes during short-term exposure of *T. mesenterina* to elevated light (days; Hoogenboom et al., 2006) as well as following longer-term reciprocal transplants of *Stylophora pistillata* across two depths (weeks to months; Cohen and Dubinsky, 2015) were subsequently characterized using repeated pulse-amplitude modulation (PAM) fluorometry. Relatively short-term (days) photoacclimation of four coral species has similarly been assessed using PAM fluorometry in combination with other metrics, such as endosymbiont cell concentration and pigment content (Langlois and Hoogenboom, 2014). Such fluorometry approaches have proven extremely critical for retrieving highly resolved photophysiological parameterization of corals over space and time (e.g. Hennige et al., 2008; Suggett et al., 2012; Langlois and Hoogenboom, 2014; Warner et al., 2010), but tying these parameters to the underlying metabolic changes that regulate photoacclimation remains challenging and largely unresolved (see Nitschke et al., 2018; Warner and Suggett, 2016).

[1]Program in Fisheries and Aquatic Sciences, School of Forest Resources and Conservation, University of Florida, Gainesville, FL 32603, USA. [2]Climate Change Cluster (C3), University of Technology Sydney, Ultimo, NSW 2007, Australia. [3]Metabolomics Australia, University of Melbourne, Parkville, VIC 3010, Australia. [4]School of Environmental and Life Sciences, University of Newcastle, Ourimbah, NSW 2258, Australia. [5]Center for Conservation, The Florida Aquarium, Apollo Beach, FL 33572, USA.

*Author for correspondence (kelohr@ufl.edu)

K.E.L., 0000-0002-3580-3431

Received 9 November 2018; Accepted 11 March 2019

Journal of Experimental Biology (2019) 222, jeb195982. doi:10.1242/jeb.195982

List of symbols and abbreviations

E_k	sub-saturation irradiance
$F_q'/F_{m'(max)}$	maximum photochemical efficiency of photosystem II
GC-MS	gas chromatography–mass spectrometry
HL	high light
LC-MS	liquid chromatography–mass spectrometry
LL	low light
PAM	pulse amplitude modulation
PAR	photosynthetically active radiation
PSII	photosystem II
$rETR_{max}$	maximum relative electron transport rate
RLC	rapid light curve

A metabolomic profile provides a snapshot of the metabolic physiological state of an organism at a given time to provide insight into changes that underpin light acclimation (Obata and Fernie, 2012; Weckwerth, 2003). Numerous metabolic processes are likely involved in photoacclimation and a vast array of small chemical compounds (metabolites) are critical to the operation of (and signaling amongst) these processes. Changes in the presence or concentration of metabolites have been shown to provide new insight into the physiological processes activated in response to external stimuli, e.g. temperature, pH (Sogin et al., 2016; Hillyer et al., 2017a, 2018) and the presence of competitors (Quinn et al., 2016) of reef-building corals. Some specific metabolites or targeted metabolite groups have also been assessed in corals during photoacclimation periods (e.g. mycosporine-like amino acids; Torres et al., 2007). Increased light dramatically alters the metabolome in algae (Davis et al., 2013), cyanobacteria (Meissner et al., 2015) and terrestrial plants (Wulff-Zottele et al., 2010; Obata and Fernie, 2012), and the response of the metabolome to both increased and decreased light has also been explored in the model plant species *Arabidopsis thaliana* (Caldana et al., 2011). However, whilst shifts in metabolite profiles of cultured Symbiodiniaceae are known to follow changes in temperature and light (Klueter et al., 2015), how the metabolome of the coral holobiont (coral host, endosymbiotic Symbiodiniaceae and associated microorganisms) changes during photoacclimation remains unknown.

Characterizing the effects of changes in light availability on coral metabolism is critical to understanding not only how corals respond to natural changes in light but also how corals fundamentally cope with light-altering stressors attributed to human activity, such as enhanced sedimentation (Bessell-Browne et al., 2017) and algal shading (Cetz-Navarro et al., 2015). Rapidly altered light conditions are also induced via increasingly popular interventional reef management strategies involving coral transplantation (e.g. Bruckner and Bruckner, 2001; Ross, 2014; Lohr et al., 2017; see also Cohen and Dubinsky, 2015). Many species of coral are clearly capable of acclimating to a wide range of light regimes (e.g. Anthony et al., 2003b, 2004; Langlois and Hoogenboom, 2014); thus, a better understanding of the rate and extent of coral photoacclimation can aid in determining the ability of corals to withstand sedimentation and shading and also tolerate transplantation to new light regimes during management interventions. We therefore conducted a fully reciprocal light exposure experiment to determine the nature and extent to which corals respond to low versus high light shifts. We assayed the time scale for photophysiological adjustment of the abundant reef flat coral *Acropora muricata* (Linnaeus 1758) using PAM fluorometry-derived acclimation metrics, and simultaneously used a metabolomics approach to evaluate whether and how metabolic adjustments were concurrent with photophysiological re-adjustment.

MATERIALS AND METHODS

Experimental design

A total of 58 *Acropora muricata* fragments at least 5 cm in length were collected from visually healthy source colonies on the reef crest and forereef at Heron Island, Great Barrier Reef (23.44°S, 151.91°E) in January 2017. Coral collections were performed under permits G15/37488.1 and G16/38534.1 issued by the Great Barrier Reef Marine Park Authority. The forereef collection site was located approximately 10 m seaward of the reef crest collection site. At both collection sites, source colonies were part of continuous thickets and discrete genets could not be identified. Instead, fragments were haphazardly collected from thickets within an area of approximately 3×3 m at each collection site. Maximum photosynthetically active radiation (PAR) was measured at each site at solar noon on a clear day using a PAR meter (4π spherical underwater quantum sensor, LI-193SA, LI-COR, Lincoln, NB, USA). Fragments collected from the reef crest (n=29) were clipped from the tops of high light (HL)-exposed thickets at 0.5–1 m (maximum PAR≈2500–3000 µmol photons m^{-2} s^{-1}). The remaining fragments (n=29) were collected from the underside of thickets that were exposed to comparatively low light (LL) at a depth of 3.5–4 m (maximum PAR≈500–1000 µmol photons m^{-2} s^{-1}). Collected HL and LL fragments were transported to the Heron Island Research Station and placed in seawater-conditioned plastic test tube racks to ensure they remained upright. Fragments were acclimated for 3 days in an outdoor direct flow-through system at sunlight intensities closely approximating those of their source environment. Irradiance levels approximating each source environment were achieved using shade cloth to approximate midday maximum light levels to corresponding values measured *in situ* at HL and LL collection sites (HL ∼2500–2600 µmol photons m^{-2} s^{-1} and LL ∼450–600 µmol photons m^{-2} s^{-1} maximum daily PAR).

To generate initial metabolomic profiles associated with each light regime prior to the application of experimental treatments and to account for any tank effect following the acclimation period, 10 fragments (5 each, HL and LL) were snap frozen in liquid nitrogen [sample groups hereafter referred to as initial HL (or LL) samples]. The remaining 48 fragments were distributed among two light treatments in six 68 l glass aquaria (n=3 aquaria per light treatment). Fragments were distributed in a fully reciprocal design such that equal numbers of fragments sourced from HL and LL environments were exposed to each light treatment (Fig. 1). This resulted in two treatment groups (LL to HL and HL to LL) and two control groups (LL control, HL control), each consisting of 12 colonies. Fragments from each source location were haphazardly assigned to each treatment tank, and were equally spaced in one test tube rack per tank. Each aquarium received 10 l min^{-1} flow-through seawater pumped directly from the reef flat where nubbins were originally sourced. Cross-calibrated temperature loggers (HOBO Pendant® UA-002-64 or UA-001-64, Onset Corporation, Bourne, MA, USA) were placed in each aquarium to monitor temperature throughout the experiment and ensure consistency across treatments.

Photophysiology

Endosymbiont photosystem II (PSII) photophysiology was assessed over a period of 21 days using a PAM fluorometer (Diving-PAM, Walz, Effeltrich, Germany) as per Nitschke et al. (2018). Immediately after dawn on days 0, 1, 3, 4, 7, 11, 15, 20 and 21 of the experiment, test tube racks containing corals were transported to an adjacent laboratory in a seawater-filled container, and rapid light curves (RLCs) with eight actinic light steps were performed on each

Journal of Experimental Biology (2019) 222, jeb195982. doi:10.1242/jeb.195982

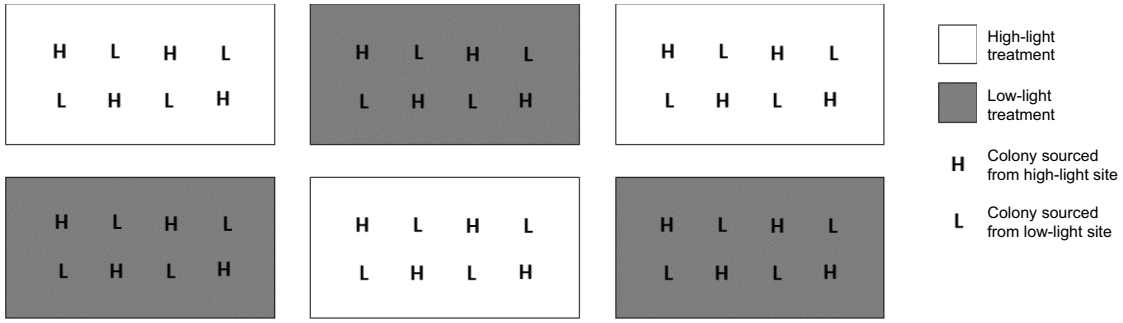

Fig. 1. Experimental design for the study. Biological replicate fragments of *Acropora muricata* sourced from high-light (H, *n*=24) and low-light (L, *n*=24) sites were equally distributed among high-light treatments (open boxes, *n*=3) and low-light treatments (shaded boxes, *n*=3). This schematic diagram illustrates the relative distribution of H- and L-sourced corals among treatment tanks, but does not represent the actual positions of treatment tanks and replicate colonies within tanks, which were haphazard. Photophysiological and metabolomic changes were assessed for replicate corals over a period of 21 days.

replicate fragment. Corals were kept under low light to remove potential artifacts from dark-induced plastoquinone reduction. Actinic light levels were calibrated with a PAR meter (4π spherical underwater quantum sensor, LI-193SA, LI-COR) prior to each set of light curves. Irradiance steps were administered in 20 s intervals (as per Hennige et al., 2008; Nitschke et al., 2018). Briefly, diving-PAM settings were: actinic light factor=1, light curve intensity=3, saturation width=0.8 s, saturation intensity=10, gain=12 and signal damping=3.

RLCs for each replicate fragment were fitted to a least squares non-linear regression model that describes the light-dependent quantum efficiency of PSII (Hennige et al., 2008):

$$F_q'/F_m' = [(F_q'/F_m'_{(max)})E_k)(1 - \exp(-E/E_k))]/E, \quad (1)$$

where E_k is sub-saturation irradiance (µmol photons m^{-2} s^{-1}), $F_q'/F_m'_{(max)}$ (dimensionless) estimates the maximum photochemical efficiency of PSII and E is PAR. RLC data were also fitted to a second least squares non-linear regression model describing light-dependent electron transport:

$$rETR = rETR_{max} \times \left[1 - \exp\left(-\alpha \times \frac{E}{rETR_{max}}\right)\right], \quad (2)$$

where α (dimensionless) is light-dependent photosynthetic rate and $rETR_{max}$ (µmol electrons m^{-2} s^{-1}) is maximum relative electron transport rate.

Metabolome profiling

In addition to the 10 initial HL and LL samples collected immediately following the acclimation period, control and treatment groups were sampled from the six tanks after 7 and 21 days for metabolome profiling. A total of *n*=24 samples were collected at each time point, and thus each source × treatment group was equally represented among samples. Samples were snap frozen in liquid nitrogen to halt metabolic activity, and stored at −80°C prior to extraction. For metabolomics analysis, experimental data for HL- and LL-exposed corals were considered separately in order to better interpret how treated colonies changed with respect to relevant initial and control groups. This resulted in comparisons between (1) LL to HL colonies, LL to LL controls, and initial HL and LL samples, and (2) HL to LL colonies, HL to HL controls, and initial HL and LL samples. Both GC-MS and LC-MS analyses were performed in order to retrieve a comprehensive set of both primary and secondary metabolite responses.

GC-MS

Gas chromatography–mass spectrometry (GC-MS) profiling was used in order to target primary metabolites (such as sugars, amino acids and organic acids; Dias et al., 2015). Metabolite extraction methods for GC-MS profiling were modified from Hillyer et al. (2016, 2017a). Metabolites were extracted using 750 µl of extraction solution (100% methanol with three internal standards: 100 µmol l^{-1} DL-valine-d8, 60 µmol l^{-1} stearic acid-d3, 60 µmol l^{-1} 5-α-cholestane) per 50 mg of sample material. An additional extraction was performed using 750 µl of 50% methanol. Samples were incubated for 20 min at 5°C and 1250 rpm in a thermomixer in the respective solvents sequentially, then centrifuged for 3 min at 20,800 ***g***. The resulting supernatant was collected and pooled; 150 µl of supernatant was then transferred into a glass vial and evaporated to dryness in a vacuum evaporator for 3 h at room temperature. Samples were derivatized by adding 20 µl of 20 mg ml^{-1} methoxylamine in pyridine then incubating samples at 37°C for 2 h at 750 rpm in the agitator. Then, 20 µl of *N*-methyl-*N*-(trimethylsilyl) trifluoroacetamide was added and samples were incubated at 37°C for 30 min at 750 rpm in the agitator. Samples were subsequently incubated at room temperature for 1 h, and finally 1 µl was injected for GC-MS analysis.

Samples were run on a GCMS-QP2020 (Shimadzu Corporation, Kyoto, Japan) equipped with an AOC-20is autosampler (Shimadzu Corporation). The column used was an SH-Rxi-5Sil MS fused silica capillary column (30.0 m×0.25 mm×0.25 µm) operating in electron impact mode at 70 eV. Helium was used as the carrier gas at a constant flow of 1.0 ml min^{-1} and an injection volume of 1 µl, with an injector temperature of 280°C and an ion source temperature of 230°C. The temperature gradient of the oven was 70°C for 1 min, then 7°C per minute to 325°C. The scan range was *m/z* 50–600. Samples were run in a randomized order to account for any potential experimental drift affecting experimental groups. A quality control (QC) sample composed of replicates from each sample group was also injected periodically.

LC-MS

Metabolite extraction methods for liquid chromatography–mass spectrometry (LC-MS) were modified from Gordon et al. (2013). Frozen coral fragments were placed in 20 ml scintillation vials containing 10 ml of 100% methanol (LC-MS Grade, BandJ Brand, Honeywell, Shanghai, China) spiked with 0.005 mmol l^{-1} aminoanthracene (Sigma-Aldrich, Castle Hill, Australia) as an internal standard, then stored at −20°C overnight. Vials were sonicated in a chilled water bath for 15 min then vortexed for 30 s per sample. Resulting extracts were decanted into clean scintillation

vials, and 3 ml of 70% methanol was added to vials containing remaining coral nubbins to ensure extraction of hydrophilic metabolites. Samples in 70% methanol were vortexed for another 30 s and the resulting extract was combined with the 100% methanol extract. The combined extract was stored at −20°C overnight. A syringe was then used to remove 1 ml of extract, which was passed through a 0.22 µm Hydraflavon syringe filter (MicroAnalytix Pty Ltd, Taren Point, Australia) to remove any particulate matter and into clean 2 ml HPLC vials. Vials were stored at −20°C overnight prior to processing.

Untargeted LC-MS metabolite profiling was conducted using a reverse phase (C18) technique targeting semi-polar to hydrophobic secondary metabolites (De Vos et al., 2007). Samples were analyzed on 6550 iFunnel Q-TOF LC-MS (Agilent Technologies, Santa Clara, CA, USA) equipped with dual automatic jet stream electrospray ionization (AJS ESI), coupled with a 1260 infinity HPLC system (Agilent Technologies). Separation was performed at 25°C on an Agilent Zorbax Eclipse XDB-C18 column (100×4.6 mm i.d., 1.8 µm). The HPLC program consisted of a linear gradient of milli-Q water (with 1% formic acid) to 100% acetonitrile (with 1% formic acid) over 12 min, followed by isocratic elution at 100% acetonitrile (with 1% formic acid) at a flow rate of 1 ml min^{-1}. Nitrogen was used as the nebulizing gas. The dual AJS ESI source was kept at a voltage of 3500 V in positive ion mode. Mass spectra were acquired with source conditions as follows: gas temperature 350°C, drying gas 4 l min^{-1} (N_2), nebulizer pressure 35 psi (N_2) and Vcap 3500 V, fragmentor 160 V and skimmer 65 V. The mass range scanned was 70–1700 *m/z*, at a scan rate of 2 spectra s^{-1}. Because analysis was untargeted, generic settings were applied to obtain as many compounds as possible. All samples were injected in a single batch and a randomized injection order was used to avoid sample mass. A QC sample composed of replicates from each sample group was analyzed at the beginning, middle and end of the batch. External mass calibration was performed using a calibrating solution monitoring signals at *m/z* in positive polarity. Data were processed using Mass Hunter Qualitative analysis software (v.B.06.00 Agilent Technologies). All solvents used were of high purity grade from Honeywell Burdick and Jackson (Chem-Supply, Gillman, Australia). LC-MS grade formic acid was obtained from Sigma-Aldrich.

Data analysis

Statistical tests were performed using a significance level of α=0.05 and means are presented ±s.e.m. Photochemical parameters retrieved from modelling PAM fluorescence light–response curves (E_k, $F_q'/F_{m'(max)}$ and $rETR_{max}$) were compared among treatments over time using linear mixed models with repeated measures. An ar(1) model was used to assess the correlation caused by repeated measures. Variance was allowed to vary by treatment. All analyses of photochemical parameters were performed using SAS statistical software (v.9.4, SAS Institute).

Raw GC-MS data were transformed into CDF format using GCMSsolution software (v.4.0, Shimadzu, Kyoto, Japan), and the converted files were subsequently imported into XCMS (v.3.2, Galaxy Project Metabolomics, Roscoff, France). XCMS software, which is freely available under an open-source license at http://metlin.scripps.edu, incorporates non-linear retention time alignment, matched filtration, peak detection and peak matching. For grouping, bandwidth was set to 10; the resulting peak list comprising features (ions, retention time, intensity) was further processed using Excel (Microsoft, Redmond, WA, USA), where area normalization was performed using the total peak area of internal standards and used for further statistical analysis. Statistical analysis of the normalized features with a unique *m/z* and retention time (mzRT) obtained from XCMS representing 182 metabolites was performed using MetaboAnalyst 4.0 software (www.metaboanalyst.ca). Normalized peak areas were log transformed and autoscaled (the mean area value of each feature throughout all samples was subtracted from each individual feature area and the result divided by the standard deviation) prior to statistical analysis. Features showing statistically significant differences among the groups were used to annotate peaks. Groups of features sharing the same retention time that were statistically significant and presented with a high degree of correlation were considered representative of a single metabolite (Escobar-Morreale et al., 2012). Metabolite profiling and tentative metabolite identification were performed using GCMSsolution software by combining mass spectra and database consultation (NIST17, match with library >70%). Further validation was also done through literature searches.

Raw LC-MS data were processed using the Batch Recursive Feature Extraction option in the Agilent Mass Hunter Profinder software (v.B.06.00). Untargeted analysis of complex biological mixtures comprises tens of thousands of mass features, and thus allows profiling of a large number of molecules. Several preprocessing filters were applied to curate the large amount of data to an operational size. Using the feature extraction algorithm, a group of ions characterized by retention time, peak area and accurate mass was extracted in each sample as molecular features. This was performed by using a minimum absolute abundance threshold of 1000 counts with an *m/z* range of 100–1700. The charge state was set to 2 and the minimum number of ions in the isotopic distribution was set to 2, following the isotope model of ‘common organic molecules’. This was followed by binning and alignment of molecular features as a function of retention time, fragmentation pattern and *m/z* value across the data matrix, using a tolerance window of ±0.1%+0.2 min retention time and ±10 ppm+2 mDa mass window. H^+, Na^+, K^+, and NH_4^+ ion species and neutral losses of H_2O and CO_2 were allowed. Next, a visual validation of the feature extraction results and manual editing of extracted ion chromatogram (EIC) peaks as required were performed using Profinder to reduce the number of false negatives and false positives in the dataset, thereby increasing the quality of the data exported for differential analysis. Data files were transformed into .CEF files containing extracted compounds, neutral mass, retention time and abundance, and exported to Mass Profiler Professional (MPP) software package (v.B.14.9.1, Agilent Technologies).

Data were normalized with the internal standard and evaluated and filtered to remove low-quality and inconsistent mass spectral features (only those appearing in 75% of samples in at least one condition were considered). Thereafter, compound abundance values in each sample were baselined to the median of each compound in all samples. Resultant mass features were exported as .csv files and statistical comparisons including principal component analysis (PCA), partial least square discriminant analysis (PLS-DA) and hierarchical cluster analysis were performed using MetaboAnalyst 4.0 software (www.metaboanalyst.ca). Statistically significant differences among sample groups were determined using one-way ANOVA and Tukey’s HSD (α=0.05) using the exported dataset.

RESULTS

Photophysiology

In contrast to previous studies (e.g. Hennige et al., 2008), values of maximum PSII photochemical efficiency ($F_q'/F_{m'(max)}$) at time

Journal of Experimental Biology (2019) 222, jeb195982. doi:10.1242/jeb.195982

zero did not vary between LL and HL fragments. Furthermore, $F_q'/F_{m'(max)}$ remained constant throughout experimentation, with no interaction between source location and time, and no clear pattern for differences among treatment groups over time (Fig. 2A,B). In contrast, changes in E_k and $rETR_{max}$ demonstrated reciprocal photoacclimation patterns for *A. muricata* (Fig. 2C,D; Fig. S1). Specifically, mean E_k for HL-sourced corals (252.25±16.18 µmol photons m^{-2} s^{-1}; Fig. 2D) was significantly greater than that of LL-sourced corals (121.44±11.19 µmol photons m^{-2} s^{-1}; Fig. 2C) at t=0 (P<0.0001). After 3 days of exposure to light treatments, there was no longer a significant difference in E_k based on source location, regardless of light treatment (P>0.05). However, by the conclusion of the experiment (t=21 days), light treatment had a significant effect on E_k, regardless of source location (P=0.01; E_k=230.08±17.83 µmol photons m^{-2} s^{-1} for LL to HL and HL to HL control corals and 143.50±8.99 µmol photons m^{-2} s^{-1} for HL to LL and LL to LL control corals), thereby demonstrating clear emergent photoacclimation responses of treated coral fragments to their new light environments.

Values for $rETR_{max}$ followed a similar pattern to those for E_k (Fig. S1). At t=0, mean $rETR_{max}$ for HL-sourced corals (94.43 ±4.67 µmol electrons m^{-2} s^{-1}) was significantly greater than that of LL-sourced corals (47.70±3.61 µmol electrons m^{-2} s^{-1}; P<0.0001). After 1 day of exposure to light treatments, $rETR_{max}$ no longer differed based on source location (P>0.05), and differed significantly based on light treatment (P=0.01). Light treatment also had a significant effect on $rETR_{max}$, regardless of source location at t=7 (P=0.01) and at the conclusion of the experiment (t=21, P<0.01). At t=21, mean $rETR_{max}$ was 90.88±5.46 µmol electrons m^{-2} s^{-1} for the LL to HL colonies and HL to HL control colonies and 58.45±3.07 µmol electrons m^{-2} s^{-1} for the HL to LL colonies and LL to LL control colonies.

Metabolomic responses to light shifts

A total of 182 metabolites were resolved by GC-MS, 59 of which were annotated by comparison to the NIST 2017 mass spectral library. PCA and PLS-DA of all mass features suggested metabolic adjustment during the 21 day experimental period (Fig. 3; Fig. S2). Initial HL and LL coral samples clustered separately in both PCA and PLS-DA models. Metabolomic profiles of LL to HL corals clustered separately from LL to LL controls at both t=7 and t=21 (Fig. 3A; Fig. S2A). PCA and PLS-DA indicated that the majority of metabolic adjustment for LL to HL corals occurred during the first 7 days of treatment, i.e. a larger shift occurred between t=0 and t=7 than between t=7 and t=21. Separation of metabolomic profiles was less distinct for HL to LL colonies and HL to HL controls (Fig. 3B; Fig. S2B). In the PCA model, HL to LL colonies clustered separately from HL to HL controls at t=7; however, overlap between HL to LL colonies and both initial HL and LL profiles was also apparent (Fig. S2B). Additionally, a great deal of overlap with control and initial groups was apparent for HL to LL colonies at t=21. PLS-DA for the same treatment and control groups illustrated that HL to LL corals at t=7 and t=21 generally clustered closer to initial LL samples; however, overlap with HL to HL control colonies was apparent at both t=7 and t=21 (Fig. 3B). Consequently, metabolomic profiles for HL to LL corals do not appear to be as distinct from HL to HL controls compared with those of LL to HL coral and LL to LL controls.

A total of 33 metabolites differed significantly between LL to LL controls and LL to HL corals. Of these metabolites, 21 were

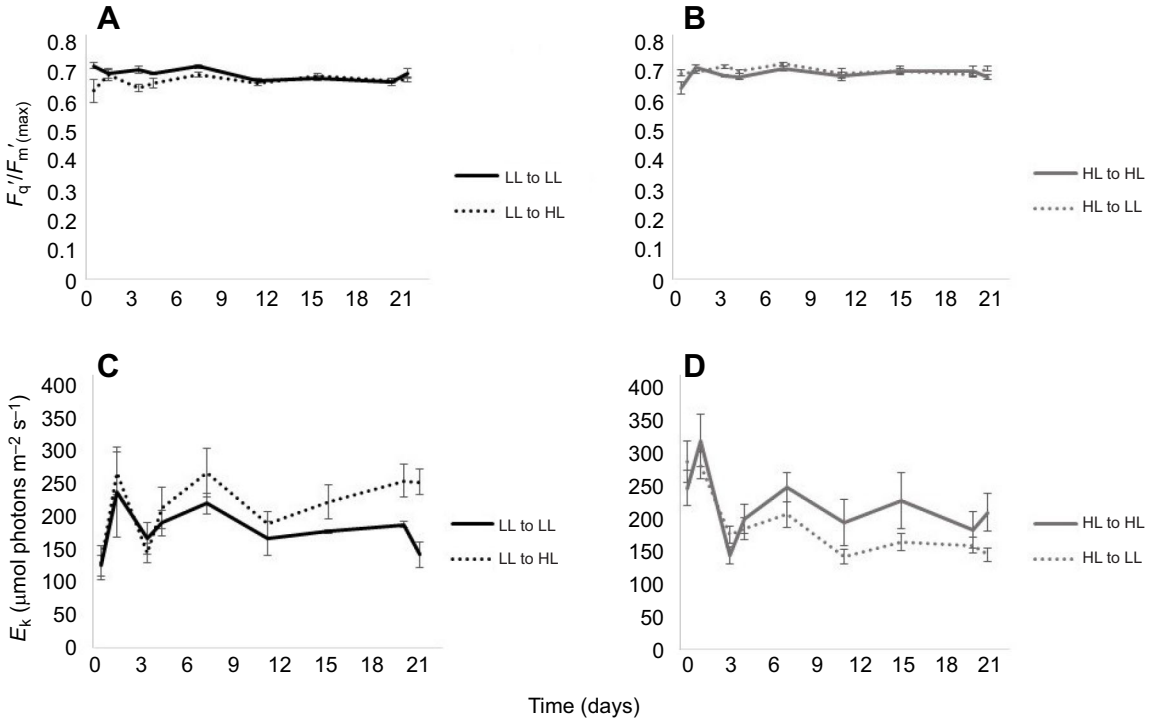

Fig. 2. Maximum photochemical efficiency of PSII ($F_q'/F_{m'(max)}$) (top) and sub-saturation irradiance (E_k) (bottom) over time. (A,C) Data for corals sourced from low-light conditions (LL, n=24) and subjected to either HL treatment (LL to HL) or LL treatment (LL to LL, control). (B,D) Data for corals sourced from high-light conditions (HL, n=24) and subjected to either LL treatment (HL to LL) or HL treatment (HL to HL, control). Data are means±s.e.m. A linear mixed model indicated treatments had no clear effect on $F_q'/F_{m'(max)}$. At t=0, a linear mixed model indicated that E_k varied significantly based on source location only (HL versus LL; P<0.0001). After 3 days of treatment, E_k did not vary significantly based on source location. By t=21, treatment had a significant effect on E_k (P=0.01), illustrating photoacclimation over time.

Journal of Experimental Biology (2019) 222, jeb195982. doi:10.1242/jeb.195982

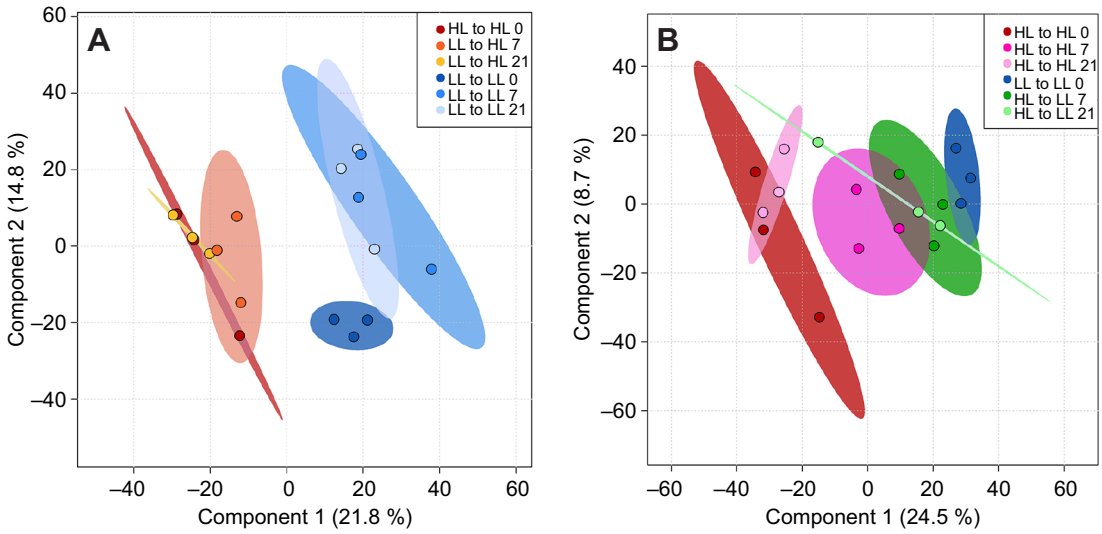

Fig. 3. Partial least square discriminant analysis (PLS-DA) models based on GC-MS data illustrating shifts in the metabolome over time for corals sourced from different light levels. (A) LL corals; (B) HL corals. Each group consisted of *n*=3 samples, and shading indicates 95% confidence intervals. Metabolomic profiles of initial HL and initial LL samples (*t*=0) were distinct (A,B). At *t*=7 and *t*=21, separation was apparent between LL to HL corals and LL to LL controls (A). LL to HL corals at both time points clustered with initial HL samples (*t*=0) (A). Although some shifts appear to have occurred for HL to LL corals, metabolomic profiles for HL to LL corals overlapped with those for HL to HL controls at *t*=7 and *t*=21 (B).

tentatively annotated using the NIST 2017 library, and included an array of amino acids, organic acids, fatty acids and sterols. Fig. 4 illustrates differences in relative concentrations of significant metabolites among treatment and control groups. Heat maps indicated two major clusters when LL to HL treatments were compared against LL to LL controls (Fig. 4A). LL to HL colonies at both *t*=7 and *t*=21 clustered with initial HL samples, while LL to LL controls clustered with initial LL samples. Discrimination between these clusters was very effective, again suggesting that most metabolic adjustment occurred within 7 days of treatment application. LL to HL colonies and initial HL samples were characterized by relatively lower concentrations of the steroid campesterol and the alcohols 1-hexanol and glycerol compared with LL to LL controls and initial LL samples. LL to HL colonies and initial HL samples also had relatively higher concentrations of the fatty acids tetradecanoic acid (C14:0) and dodecanoic (C12:0) acid, the amino acid L-cysteine and the alcohol 1-hexadecanol compared with LL to LL controls and initial LL samples. Although a number of significant metabolites were also identified for HL to LL colonies compared with HL to HL controls and HL and LL initial samples, there was no clear clustering pattern among treatment, control and initial sample groups (Fig. 4B). These results suggest that light exposure over the 21 day experimental period did not have a clear effect on metabolite concentrations among HL to LL treatment, HL to HL control, and HL and LL initial sample groups.

Based on mass accuracy and retention time, 1175 molecular features were aligned across the LC-MS retrieved sample set, and this number was reduced to 1090 molecular features after filtering by frequency (see Materials and Methods). A total of 28 molecular features were found to be statistically different between LL to HL treatment and LL to LL control groups. PCA and PLS-DA models based on LC-MS molecular features generally demonstrated metabolic adjustment during the 21 day experimental period (Fig. 5; Fig. S3). Initial HL and LL samples clustered separately in both PCA and PLS-DA models. PCA indicated overlap in the metabolomes of LL to HL corals and LL to LL controls at *t*=7; however, treatment and control profiles were distinct by *t*=21 (Fig. S3A). PLS-DA showed distinct clustering of LL to HL corals and LL to LL controls at all time points (Fig. 5A). In contrast to PCA, PLS-DA indicated that the majority of (LC-MS) metabolic adjustment for LL to HL corals occurred during the first 7 days of treatment, with a larger shift occurring between *t*=0 and *t*=7 than between *t*=7 and *t*=20 (Fig. 5A). Overlap between HL to LL colonies and HL to HL controls was apparent at both time points in the PCA model (Fig. S3B). Separation of metabolomic profiles was less distinct for HL to LL colonies and HL to HL controls in the PLS-DA model (Fig. 5B). While HL to LL corals at *t*=7 and *t*=21 generally clustered closer to initial LL samples, overlap with HL to HL controls was also apparent at each time point, indicating that metabolomic shifts resulting from the HL to LL treatment were less substantial than those associated with the LL to HL treatment. Heat maps resolved two major clusters when significant molecular features were compared for LL to HL versus LL to LL controls (Fig. 6). LL to HL treatments at both *t*=7 and *t*=21 clustered with initial HL samples, while LL controls and initial LL samples formed a separate cluster. Discrimination between these clusters was very effective, again suggesting that most metabolomic changes occurred within 7 days of treatment. No molecular features were found to vary significantly between HL to LL treatment groups and HL to HL controls. Fig. S4 illustrates the number of features identified by LC-MS that were found to change over time in LL to HL corals versus HL to LL corals.

DISCUSSION

Coral photoacclimation properties and how they vary over space and time have become increasingly well studied (e.g. Anthony and Hoegh-Guldberg, 2003a; Frade et al., 2008), particularly through the introduction of highly resolute bio-optical techniques such as PAM fluorometry (Hennige et al., 2008; Nitschke et al., 2018). However, associated metabolic changes that regulate cellular physiological processes inherent to photoacclimation in the coral holobiont have not been comprehensively explored. Our present study therefore applied coupled photophysiology and metabolomic measurements for the first time to generate new insight into the

Journal of Experimental Biology (2019) 222, jeb195982. doi:10.1242/jeb.195982

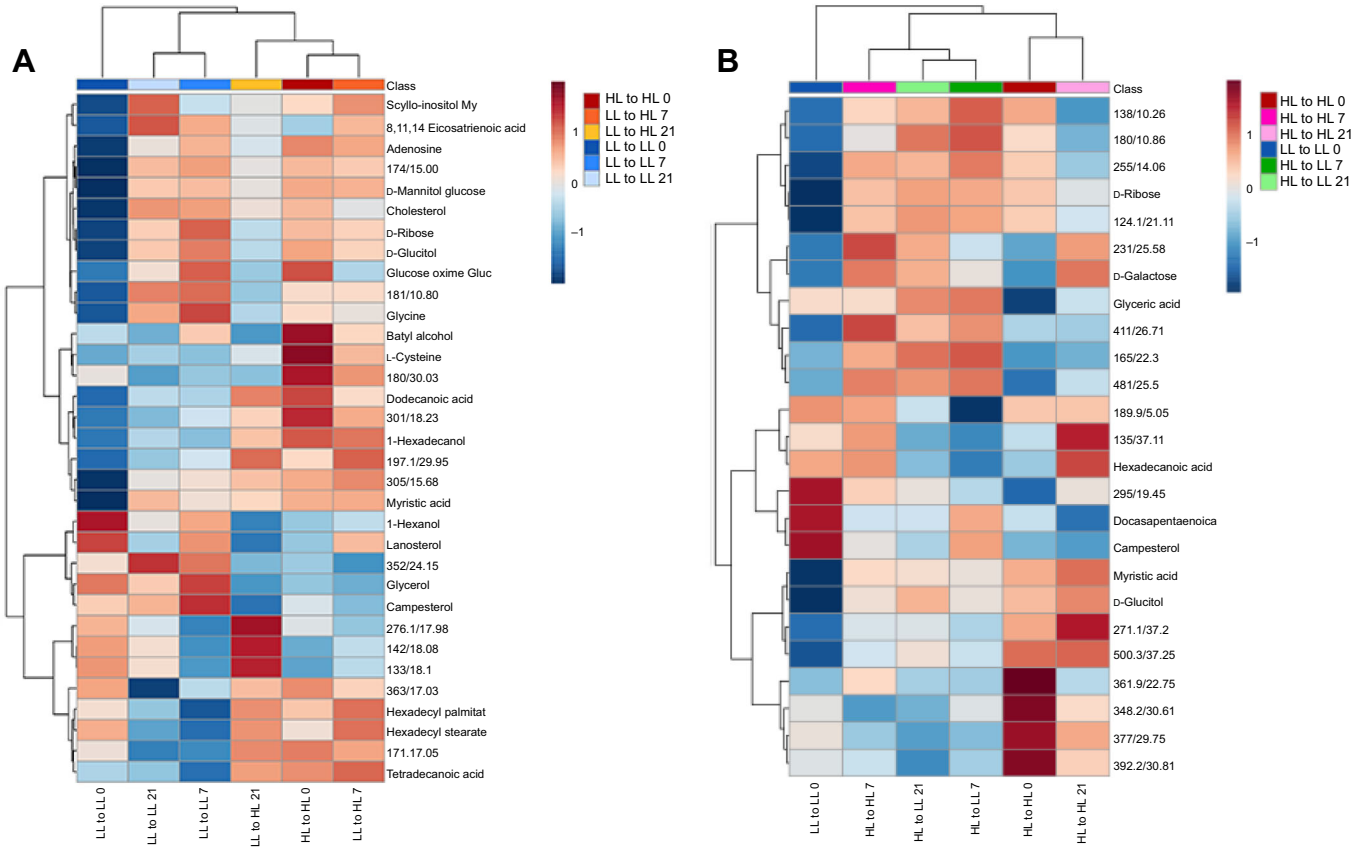

Fig. 4. Heat maps comparing significant entities identified by GC-MS and ANOVA for corals sourced from different light levels. (A) LL corals; (B) HL corals. Each group consisted of *n*=3 samples. Individual entities are presented using tentative annotations or mass/retention time for compounds that were not annotated. (A) The 33 entities that were found to vary significantly among groups using ANOVA ($P<0.05$). Two major clusters that were resolved based on relative concentrations of significant entities are shown: LL to HL corals at both $t=7$ and $t=21$ cluster with HL to HL controls at $t=0$, while LL to LL controls at all time points cluster separately. These results suggest that substantial metabolic adjustment occurred among LL to HL corals. (B) Here, 25 metabolites were found to vary significantly among groups using ANOVA ($P<0.05$). However, there was no clear clustering based on significant entities among HL to LL corals and HL to HL controls. These results suggest that the effect of reduced light on the metabolome of *A. muricata* was less substantial during the 21 day study period compared with the effect of increased light.

biology of coral photoacclimation. Consistent with previous studies, corals were able to acclimate to both increases and decreases in light availability (Falkowski and Dubinsky, 1981; Cohen and Dubinsky, 2015) during the time frame of our experiment. Changes in photophysiological parameters, notably the light intensity for saturated photosynthesis (E_k) and maximum electron transport rate ($rETR_{max}$), but not maximum photochemical efficiency of PSII ($F_q'/F_{m'(max)}$), suggest photoacclimation in these shallow reef flat *Acropora muricata* occurred primarily through changes in capacity for maximum photosynthesis rather than light harvesting (Hennige et al., 2008; Suggett et al., 2012). Furthermore, metabolomic shifts were observed within 7 days of treatment, particularly following high light exposure, suggesting a link between metabolite profile and photoacclimation response.

The lack of change observed for $F_q'/F_{m'(max)}$ contrasts with results from a number of previous studies, which report concurrent shifts in $F_q'/F_{m'(max)}$ with shifts in light (Hennige et al., 2008; Warner et al., 2010; Suggett et al., 2012; Nitschke et al., 2018). This result is particularly intriguing, as other metrics (i.e. E_k, $rETR_{max}$) clearly indicate photoacclimation occurred during the study period. Although these results appear conflicting, one possible explanation is that $F_q'/F_{m'(max)}$ is modified by a complex interaction of active PSII reaction centers versus absorption characteristics. For example, opposing responses of enhanced photoprotection through more heat dissipation of absorbed light (reduced photochemical efficiency) coupled with parallel increases in the proportion of active PSII centers (enhanced photochemical efficiency) to drive photochemistry more efficiently per unit photon absorbed (Suggett et al., 2009) would yield a net outcome of a relatively constant $F_q'/F_{m'(max)}$. This notion is supported by previous findings of intracolonial variation in both light absorption (Kaniewska et al., 2008; Wangpraseurt et al., 2012) and photosynthetic activity (Ralph et al., 2002), but whether a similar mechanism drives the relatively constant $F_q'/F_{m'(max)}$ in the present study cannot currently be resolved and clearly warrants more targeted investigation.

Other photophysiological adjustments following changes in light availability are more consistent with a number of findings from previous studies. Increases in E_k and $rETR_{max}$ with increasing light were also found for *Porites lutea* (Hennige et al., 2008) and various Brazilian coral species (Suggett et al., 2012) growing at different depths. In our dynamic light shift experiment, E_k did not vary significantly until day 21, consistent with previous reports of no change to E_k in *A. muricata* following 9 days of exposure to both increased and decreased light (Langlois and Hoogenboom, 2014). In contrast, Anthony and Hoegh-Guldberg (2003a) estimated that E_k could adjust and reach stable values within 5–10 days in *Turbinaria mesenterina*, far shorter than the time required for adjustment in *A. muricata*. This may be a result of species-specific

Journal of Experimental Biology (2019) 222, jeb195982. doi:10.1242/jeb.195982

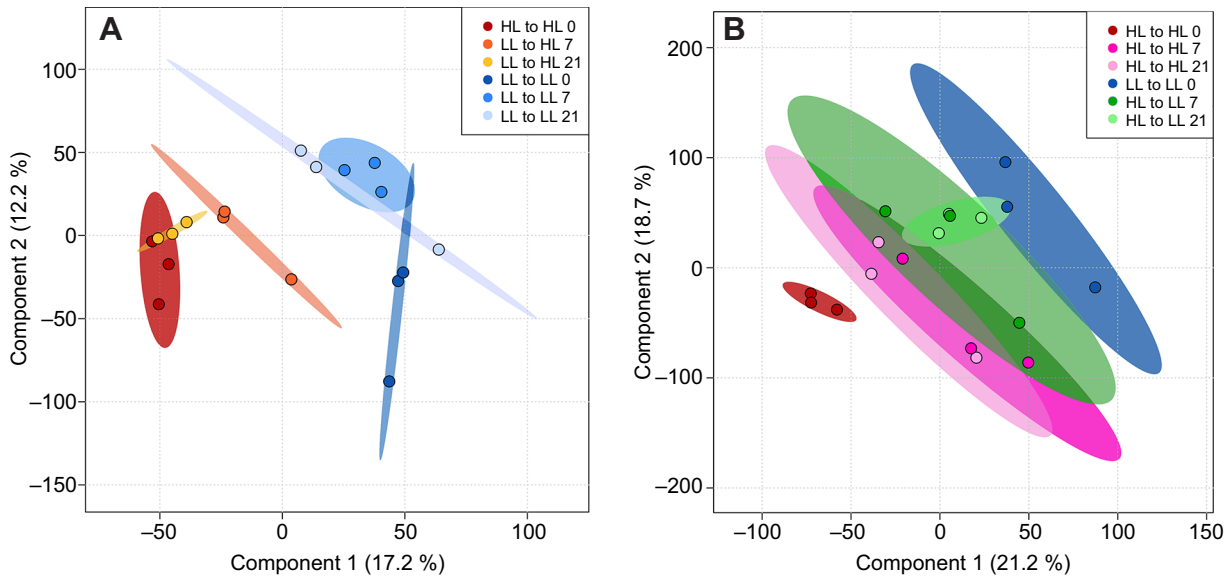

Fig. 5. PLS-DA models based on LC-MS data illustrating shifts in the metabolome over time for corals sourced from different light levels. (A) LL corals; (B) HL corals. Each group consisted of *n*=3 samples, and shading indicates 95% confidence intervals. Metabolomic profiles of HL to HL and LL to LL samples at *t*=0 were distinct (A,B). At *t*=7 and *t*=21, separation was apparent between LL to HL corals and LL to LL controls (A). LL to HL corals at both time points clustered with initial HL samples (*t*=0) (A). Although some shifts appear to have occurred for HL to LL corals, metabolomic profiles for HL to LL corals overlapped with those for HL to HL controls at *t*=7 and *t*=21 (B).

differences in photoacclimation capacity or rate, which could relate to colony morphology (Nitschke et al., 2018). Specifically, *T. mesenterina* has a plating growth form that results in continuous exposure of a high percentage of its polyps to altered light regimes; in contrast, many *A. muricata* polyps are oriented at angles up to 90 deg to incident irradiance, resulting in less consistent exposure of the colony to a given light regime, and potentially a lengthier acclimation period. Alternatively, the lack of change in E_k reported by Langlois and Hoogenboom (2014) may reflect combined effects of photoinhibition and acclimation over increased light levels (i.e. the capacity for photoacclimation in *A. muricata* was exceeded).

Intriguingly, Langlois and Hoogenboom (2014) also found no variation in $rETR_{max}$ among *A. muricata* during their 9 day acclimation period, which contrasts with our observations of changes in $rETR_{max}$ after 1 day of exposure to treatment light in the present study. Such contrasting findings may result from the fact that the highest and lowest light treatment in Langlois and Hoogenboom (2014) differed by only 905 µmol photons m^{-2} s^{-1}, whereas the treatments in the present study differed by ∼2000 µmol photons m^{-2} s^{-1}. More substantial differences in light treatments in the present study may have elicited a greater photophysiological response in *A. muricata*. Contrasting results have been reported from studies of other coral species. Although increases in E_k for deep-water *Stylophora pistillata* transplanted to a shallow site agreed with the findings of our study, E_k was also found to increase for shallow-water colonies transplanted to deeper sites after 14 days, suggesting a lack of short-term acclimation to reduced light (Cohen and Dubinsky, 2015). However, after 6 months, E_k for deep-water *S. pistillata* transplanted to a shallow site decreased to levels similar to E_k of deep-water control colonies (Cohen and Dubinsky, 2015). This indicates that susceptibility to photoinhibition can increase with time in corals moved to high light environments (Cohen and Dubinsky, 2015), and broadly suggests that observed photoacclimation may be temporary in some cases. Repeated photophysiological measurements at regular intervals over a longer study period (i.e. months) are therefore likely required to resolve the stability of adjustments to E_k in *A. muricata*.

Although photophysiological parameters changed within a relatively short time frame of 21 days, metabolomic shifts were resolved using PLS-DA within an even faster period of 7 days, particularly for LL to HL corals. Importantly, metabolomic shifts were apparent well before any significant differences in E_k and $rETR_{max}$ were observed. This indicates that metabolic reorganization occurs very shortly after a light shift, and that the emergent 'signatures' detected by PAM are an endpoint of these shifting metabolic processes, and hence only detected well into the photoacclimation process. This is consistent with the findings of a study by Hawkins et al. (2014), which documented cellular-level responses to thermal stress in symbionts well before bleaching was observed. Paired metabolomic and photophysiological data therefore suggest that metabolites may be more precise biomarkers of fine-scale physiological changes during short-term photoacclimation. Although metabolomic shifts suggest a number of pathways are likely altered to achieve photoacclimation, it is unclear whether rapid adjustment is possible for all physiological responses in corals. For example, calcification rates for corals transplanted across depths remained significantly lower than those of control corals at the same depths for up to 6 months post-transplant (Cohen and Dubinsky, 2015). Again, longer-term studies could better address the effects of rapid light shifts on *A. muricata* characteristics that may require a longer study period to exhibit a response, such as calcification and growth.

In order to fully characterize the effect of light shifts on the *A. muricata* metabolome, we paired GC-MS and LC-MS metabolomic profiling approaches. GC-MS is well recognized as a useful method for identifying primary metabolites with low molecular weight, such as sugars, fatty acids and amino acids (De Vos et al., 2007; Liu et al., 2017). An advantage of GC-MS is that it is highly reproducible, and a number of libraries have been developed to facilitate identification of primary metabolites (De Vos et al., 2007; Lee et al., 2013). In contrast, LC-MS is more beneficial

Journal of Experimental Biology (2019) 222, jeb195982. doi:10.1242/jeb.195982

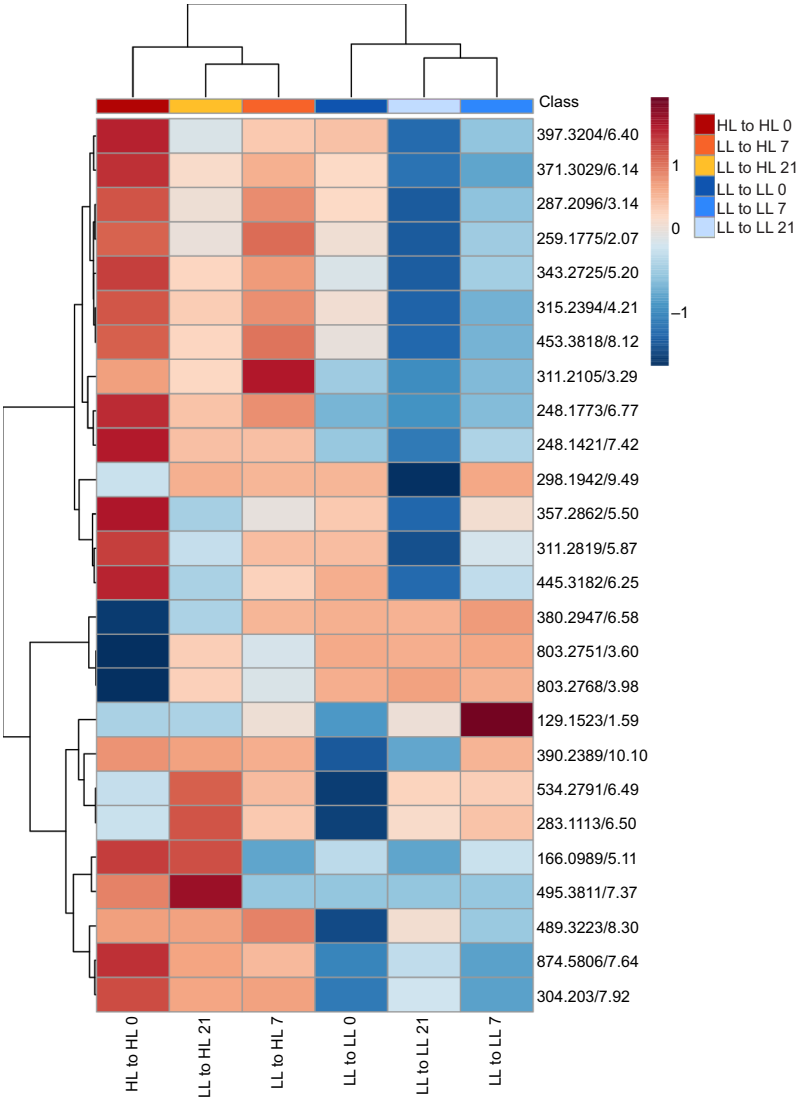

Fig. 6. Heat map comparing significant entities identified by LC-MS and ANOVA for corals sourced from LL. Each group consisted of n=3 samples. Individual entities are presented as mass/retention time. Twenty-six entities were found to vary significantly among groups using ANOVA (P<0.05). Two major clusters were resolved based on relative concentrations of significant entities: LL to HL corals at both t=7 and t=21 cluster with HL to HL controls at t=0, while LL to LL controls at all time points cluster separately. These results suggest that substantial metabolic adjustment occurred among LL to HL corals.

for distinguishing secondary metabolites, such as terpenoids, alkaloids and phenols (De Vos et al., 2007; Liu et al., 2017). Because secondary metabolites are often species specific (Lee et al., 2013), their identification can be far more challenging, particularly in the absence of species-specific metabolite databases. Identification of molecular features resolved using LC-MS therefore typically requires subsequent application of targeted approaches such as tandem MS (Viant et al., 2017), which was beyond the scope of the present study. To facilitate future elucidation of the 28 primary targets of interest from the LC-MS analysis, the raw data, including composite spectra, were submitted to MetaboLights (see 'Data availability', below). Regardless, the use of GC-MS and LC-MS approaches in concert offers a more complete picture of metabolomic adjustment during photoacclimation than either approach could offer alone. The findings of this study are also strengthened by the fact that overall metabolomic trends were comparable between approaches.

GC-MS and LC-MS metabolomic profiling approaches also differ in the total number of metabolites they typically retrieve. In the present study, >1000 molecular features were found among samples using LC-MS profiling. The high number of features retrieved using LC-MS is generally consistent with previous studies of corals; for example, Farag et al. (2016) reported >6000 mass signals among five species of the soft coral genus *Sarcophyton*. In contrast, GC-MS profiling detected 182 metabolites, 59 of which were annotated by comparison to the NIST 17 library. This is generally comparable to previous GC-MS studies of corals and their symbionts; for example, Klueter et al. (2015) detected a total of 188 metabolites among Symbiodiniaceae samples, 110 of which were identified to at least the level of metabolite class. Hillyer et al. (2017a) identified 66 unique metabolites among *A. aspera* host samples and 73 metabolites among isolated symbiont samples, and Matthews et al. (2017) identified 89 compounds in the host tissue of the cnidarian *Exaiptasia pallida*.

Both GC-MS and LC-MS approaches revealed overlap between metabolomic profiles of HL to LL corals and HL to HL controls. This finding indicates that the metabolome of HL to LL corals did not shift substantially, particularly compared with LL to HL corals. This could suggest fewer metabolic pathways are altered in response to reduced light availability. Acclimation to high light generally requires rapid photoprotective responses to minimize oxidative stress and repair PSII damage (Lesser and Shick, 1989; Jeans et al., 2013), which could reasonably manifest in a larger and more rapid metabolic change compared with low light acclimation. In contrast, low light acclimation generally consists of increases in symbiont and/or photosynthetic pigment density (Falkowski and Dubinsky,

1981; Titlyanov et al., 2001; Jeans et al., 2013; Langlois and Hoogenboom, 2014). While changes in pigment density can occur rapidly, nearly 6 weeks were required to observe significant changes in symbiont density in *Stylophora pistillata* (Titlyanov et al., 2001). Similarly, Falkowski and Dubinsky (1981) found that *S. pistillata* requires up to 8 weeks to acclimate to reduced light, approximately twice the time required to acclimate to high light in the same study. The lack of metabolomic adjustment in *A. muricata* in the present study could therefore suggest that this species also requires longer than 21 days to complete metabolic adjustments required for low-light acclimation. A lengthier acclimation period following low-light exposure could partially explain reports of initially high mortality following *in situ* transplantation of acroporid corals to lower light environments (Ross, 2014; Lohr et al., 2017). Consequently, careful consideration should also be given to selection of deeper sites during coral transplantation activities. Additionally, techniques that could aid in facilitating acclimation, such as phased transfer to deeper depths, should be explored. Future studies should also consider analyzing the host and symbiont metabolomes separately (see Hillyer et al., 2017a) in order to elucidate any metabolomic responses of either partner during low-light acclimation that could be confounded when exploring the holobiont metabolome as a whole.

In contrast to HL to LL corals, LL to HL corals underwent substantial metabolic adjustment, and their metabolomes were distinct from LL to LL controls and similar to those of initial HL samples after both 7 and 21 days of treatment. Although limited data on the effects of light on the coral metabolome are available, our findings of metabolomic variation between LL to HL colonies and LL to LL controls are supported by existing literature on photosynthetic organisms. Broad differences in metabolomic profiles were reported for the model plant species *Arabidopsis thaliana* grown under three varying light conditions (Jänkänpää et al., 2012). Similarly, a study by Klueter et al. (2015) reported differences among metabolomes of four Symbiodiniaceae species cultured under three light levels in the absence of a coral host. Glycerol was found to be a key driver of metabolomic variation among Symbiodiniaceae exposed to differing light levels (Klueter et al., 2015); this is consistent with our results, as glycerol was significantly more abundant in LL to LL controls compared with LL to HL corals at both time points (Fig. 4A). Studies of *in vitro* Symbiodiniaceae suggest glycerol may be an important photosynthetic product transferred to host organisms (Muscatine, 1967; Muscatine and Cernichiari, 1969; Suescún-Bolívar et al., 2012; Klueter et al., 2015). Lower concentrations of glycerol in LL to HL corals compared with LL to LL controls could therefore potentially indicate negative effects of HL exposure on photosynthetic processes. Hoogenboom et al. (2006) noted reduced carbon fixation by high light-acclimated corals compared with colonies acclimated to lower light levels, primarily as a result of lower chlorophyll concentration combined with higher E_k and respiration. Acclimation to HL was associated with increased E_k in the present study (Fig. 2C); however, chlorophyll concentration and respiration were not assessed. Such direct measurements of coral metabolism could help improve understanding of the potential effects of high light on carbon fixation and translocation. Furthermore, there is also evidence to suggest that studies of *in vitro* Symbiodiniaceae may overestimate the importance of glycerol, and glucose is in fact the major photosynthate translocated from *in hospite* symbionts to hosts (Ishikura et al., 1999; Hillyer et al., 2017b; Matthews et al., 2017). Glucose concentration was not found to vary between LL to HL and LL to LL control corals in the present study. However, campesterol, a compound that is known to be produced only by Symbiodiniaceae and translocated to the coral host (Treignier et al., 2009; Crandall et al., 2016), was less abundant among LL to HL samples compared with LL to LL controls. Reduced synthesis of campesterol therefore supports a potential adverse effect of high light on symbionts, and warrants further investigation.

In addition to a decrease in glycerol among LL to HL samples compared with LL to LL controls, two saturated fatty acids, tetradecanoic acid (C14:0) and dodecanoic acid (C12:0), increased in these treated samples compared with controls. Hillyer et al. (2017a) reported increases in the same fatty acids for *in hospite* Symbiodiniaceae exposed to heat stress compared with those from colonies kept in ambient conditions. Similarly, Matthews et al. (2017) found differences in fatty acids between *E. pallida* colonized with two differing symbionts. Both Hillyer et al. (2017a) and Matthews et al. (2017) suggested that accumulation of fatty acids could result from increased breakdown of lipid stores as an alternative source of energy. This could also be occurring among LL to HL corals in the present study, particularly given the concurrent reduction in the abundance of at least one metabolite known to be exclusively translocated from symbiont to host (i.e. campesterol) for this treatment group. Less information is available on the potential roles of additional metabolites that varied between LL to HL treatment and LL to LL control colonies, including 1-hexanol, L-cysteine and 1-hexadecanol. However, Shinzato et al. (2011) noted that *Acropora* corals cannot synthesize their own cysteine, and are therefore reliant on their symbionts for this amino acid. The observed increase in L-cysteine in LL to HL corals compared with LL to LL controls is therefore also likely a result of altered symbiont activity.

Metabolomic profiling, in conjunction with PAM fluorometry, provides new information on physiological changes that occur during the coral photoacclimation process. Although photophysiological datasets support findings of significant acclimation to high and low light within 21 days in *A. muricata*, paired metabolomic data suggest metabolic reorganization (particularly in LL to HL corals) begins well before acclimation is detected using fluorometry techniques. Interestingly, although E_k and $rETR_{max}$ changed significantly for corals exposed to both increased and decreased light, treatment did not have a clear effect on $F_q'/F_{m'(max)}$, contrasting with a number of previous studies. The precise mechanisms maintaining relatively constant $F_q'/F_{m'(max)}$ values over time in high and low light regimes warrant further study. Despite changes in E_k and $rETR_{max}$ for HL to LL colonies, metabolomes for this treatment group overlapped considerably with those for HL to HL controls, suggesting limited alteration of metabolic pathways following LL exposure over 21 days. In contrast, distinct photophysiological and metabolomic differences were observed between LL to HL colonies and LL to LL controls. Changes in the abundance of glycerol, campesterol and two fatty acids suggest translocation of photosynthetic products from symbiont to host may be reduced following LL to HL shifts, despite apparently successful acclimation reflected by photophysiological parameters. These metabolites could therefore prove to be useful indicators to assess the effects of rapid changes in light history, and targeted metabolomic profiling approaches could improve our understanding of how these may change over time following changes in light availability. This study improves our understanding of coral photobiology through metabolomic profiling of rapid and fine-scale metabolic changes that may not be resolved using fluorometry-based approaches alone.

Acknowledgements
The authors are grateful to the staff of the University of Queensland Heron Island Research Station for logistical support and to Gus Fordyce for field assistance.

We also thank the UF/IFAS Statistical Consulting Unit for assistance with data analysis and Joseph Henry for assistance with figure preparation.

Competing interests
The authors declare no competing or financial interests.

Author contributions
Conceptualization: K.E.L., E.F.C., W.L., J.T.P., D.J.S.; Methodology: K.E.L., E.F.C., U.K., A.L., J.T.P., D.J.S.; Formal analysis: K.E.L., U.K.; Investigation: K.E.L., E.F.C., U.K.; Resources: W.L., D.J.S.; Data curation: K.E.L., U.K.; Writing - original draft: K.E.L., E.F.C., U.K., D.J.S.; Writing - review & editing: K.E.L., E.F.C., U.K., A.L., W.L., J.T.P., D.J.S.; Visualization: K.E.L., U.K.; Supervision: E.F.C., W.L., J.T.P., D.J.S.; Project administration: E.F.C., W.L., D.J.S.; Funding acquisition: K.E.L., W.L., J.T.P., D.J.S.

Funding
This work was supported by the Australian Research Council (DP160100271 to D.J.S. and W.L.), with additional support through an Australian Research Council Future Fellowship (FT130100202 to D.J.S.). Supplemental support was provided by the University of Florida Foundation.

Data availability
Raw data from this study are available from the MetaboLights database: https://www.ebi.ac.uk/metabolights/MTBLS768.

Supplementary information
Supplementary information available online at
http://jeb.biologists.org/lookup/doi/10.1242/jeb.195982.supplemental

References
Anthony, K. R. N. and Hoegh-Guldberg, O. (2003a). Kinetics of photoacclimation in corals. *Oecologia* **134**, 23-31.
Anthony, K. R. N. and Hoegh-Guldberg, O. (2003b). Variation in coral photosynthesis, respiration and growth characteristics in contrasting light microhabitats: an analogue to plants in forest gaps and understoreys? *Funct. Ecol.* **17**, 246-259.
Anthony, K. R. N., Ridd, P. V., Orpin, A. R., Larcombe, P. and Lough, J. (2004). Temporal variation of light availability in coastal benthic habitats: Effects of clouds, turbidity, and tides. *Limnol. Oceanogr.* **49**, 2201-2211.
Bessell-Browne, P., Negri, A. P., Fisher, R., Clode, P. L. and Jones, R. (2017). Impacts of light limitation on corals and crustose coralline algae. *Sci. Rep.* **7**, 1-12.
Bruckner, A. and Bruckner, R. (2001). Condition of restored *Acropora palmata* fragments off Mona Island, Puerto Rico, 2 years after the Fortuna Reefer ship grounding. *Coral Reefs* **20**, 235-243.
Caldana, C., Degenkolbe, T., Cuadros-Inostroza, A., Klie, S., Sulpice, R., Leisse, A., Steinhauser, D., Fernie, A. R., Willmitzer, L. and Hannah, M. A. (2011). High-density kinetic analysis of the metabolomic and transcriptomic response of *Arabidopsis* to eight environmental conditions. *Plant. J.* **67**, 869-884.
Cetz-Navarro, N. P., Qua-Young, L. I. and Espinoza-Avalos, J. (2015). Morphological and community changes of turf algae in competition with corals. *Sci. Rep.* **5**, 1-12.
Cohen, I. and Dubinsky, Z. (2015). Long term photoacclimation responses of the coral *Stylophora pistillata* to reciprocal deep to shallow transplantation: photosynthesis and calcification. *Front. Mar. Sci.* **2**, 1-13.
Crandall, J. B., Teece, M. A., Estes, B. A., Manfrino, C. and Ciesla, J. H. (2016). Nutrient acquisition strategies in mesophotic hard corals using compound specific stable isotope analysis of sterols. *J. Exp. Mar. Bio. Ecol.* **474**, 133-141.
Davis, M. C., Fiehn, O. and Durnford, D. G. (2013). Metabolic acclimation to excess light intensity in *Chlamydomonas reinhardtii*. *Plant. Cell. Environ.* **36**, 1391-1405.
De Vos, R. C. H., Moco, S., Lommen, A., Keurentjes, J. J. B., Bino, R. J. and Hall, R. D. (2007). Untargeted large-scale plant metabolomics using liquid chromatography coupled to mass spectrometry. *Nat. Protoc.* **2**, 778-791.
Dias, D. A., Hill, C. B., Jayasinghe, N. S., Atieno, J., Sutton, T. and Roessner, U. (2015). Quantitative profiling of polar primary metabolites of two chickpea cultivars with contrasting responses to salinity. *J. Chromatogr. B* **1000**, 1-13.
Enríquez, S., Méndez, E. R. and Iglesias-Prieto, R. (2005). Multiple scattering on coral skeletons enhances light absoprtion by symbiotic algae. *Limnol. Ocean.* **50**, 1025-1032.
Escobar-Morreale, H. F., Samino, S., Insenser, M., Vinaixa, M., Luque-Ramírez, M., Lasunción, M. A. and Correig, X. (2012). Metabolic heterogeneity in polycystic ovary syndrome is determined by obesity: Plasma metabolomic approach using GC-MS. *Clin. Chem.* **58**, 999-1009.
Falkowski, P. G. and Dubinsky, Z. (1981). Light-shade adaptation of *Stylophora pistillata*, a hermatypic coral from the Gulf of Eilat. *Nature* **289**, 172-174.
Farag, M. A., Porzel, A., Al-Hammady, M. A., Hegazy, M. F., Meyer, A., Mohamed, T. A., Westphal, H. and Wessjohann, L. A. (2016). Soft corals biodiversity in the Egyptian Red Sea: a comparative MS and NMR metabolomics approach of wild and aquarium grown species. *J. Proteome Res.* **15**, 1274-1287.
Frade, P. R., Bongaerts, P., Winkelhagen, A. J. S., Tonk, L. and Bak, R. P. M. (2008). In situ photobiology of corals over large depth ranges: A multivariate analysis on the roles of environment, host, and algal symbiont. *Limnol. Oceanogr.* **53**, 2711-2723.
Gates, R. D. and Edmunds, P. (1999). The physiological mechanisms of acclimatization in tropical reef corals. *Am. Zool.* **39**, 30-43.
Gordon, B. R., Leggat, W. and Motti, C. A. (2013). Extraction protocol for nontargeted NMR and LC-MS metabolomics-based analysis of hard coral and their algal symbionts. In *Metabolomics Tools for Natural Product Discovery: Methods and Protocols, Methods in Molecular Biology* (ed. U. Roessner and D.A. Dias), pp. 129-147. Berlin: Springer Science and Business Media.
Hawkins, T. D., Krueger, T., Becker, S., Fisher, P. L. and Davy, S. K. (2014). Differential nitric oxide synthesis and host apoptotic events correlate with bleaching susceptibility in reef corals. *Coral Reefs* **33**, 141-153.
Hennige, S. J., Smith, D. J., Perkins, R., Consalvey, M., Paterson, D. M. and Suggett, D. J. (2008). Photoacclimation, growth and distribution of massive coral species in clear and turbid waters. *Mar. Ecol. Prog. Ser.* **369**, 77-88.
Hennige, S., Smith, D. J., Walsh, S.-J., McGinley, M. P., Warner, M. E. and Suggett, D. J. (2010). Acclimation and adaptation of scleractinian coral communities along environmental gradients within an Indonesian reef system. *J. Exp. Mar. Bio. Ecol.* **391**, 143-152.
Hillyer, K. E., Dias, D. A., Lutz, A., Wilkinson, S. P., Roessner, U. and Davy, S. K. (2017a). Metabolite profiling of symbiont and host during thermal stress and bleaching in the coral *Acropora aspera*. *Coral Reefs* **36**, 105-118.
Hillyer, K. E., Dias, D. A., Lutz, A., Roessner, U. and Davy, S. K. (2017b). Mapping carbon fate during bleaching in a model cnidarian symbiosis: the application of ^{13}C metabolomics. *New Phytol.* **214**, 1551-1562.
Hillyer, K. E., Tumanov, S., Villas-Bôas, S. and Davy, S. K. (2016). Metabolite profiling of symbiont and host during thermal stress and bleaching in a model cnidarian–dinoflagellate symbiosis. *J. Exp. Biol.* **219**, 516-527.
Hillyer, K. E., Dias, D., Lutz, A., Roessner, U. and Davy, S. K. (2018). ^{13}C metabolomics reveals widespread change in carbon fate during coral bleaching. *Metabolomics* **14**, 1-9.
Hoogenboom, M. O., Anthony, K. R. N. and Connolly, S. R. (2006). Energetic cost of photoinhibition in corals. *Mar. Ecol. Prog. Ser.* **313**, 1-12.
Iglesias-Prieto, R., Beltran, V. H., LaJeunesse, T. C., Reyes-Bonilla, H. and Thomé, P. E. (2004). Different algal symbionts explain the vertical distribution of dominant reef corals in the eastern Pacific. *Proc. R. Soc. B Biol. Sci.* **271**, 1757-1763.
Ishikura, M., Adachi, K. and Maruyama, T. (1999). Zooxanthellae release glucose in the tissue of a giant clam, *Tridacna crocea*. *Mar. Biol.* **133**, 665-673.
Jänkänpää, H. J., Mishra, Y., Schröder, W. P. and Jansson, S. (2012). Metabolic profiling reveals metabolic shifts in *Arabidopsis* plants grown under different light conditions. *Plant Cell Environ.* **35**, 1824-1836.
Jeans, J., Campbell, D. A. and Hoogenboom, M. O. (2013). Increased reliance upon photosystem II repair following acclimation to high-light by coral-dinoflagellate symbioses. *Photosynth. Res.* **118**, 219-229.
Kaniewska, P., Anthony, K. R. N. and Hoegh-Guldberg, O. (2008). Variation in colony geometry modulates internal light levels in branching corals, *Acropora humilis* and *Stylophora pistillata*. *Mar. Biol.* **155**, 649-660.
Klueter, A., Crandall, J. B., Archer, F. I., Teece, M. A. and Coffroth, M. A. (2015). Taxonomic and environmental variation of metabolite profiles in marine dinoflagellates of the genus *Symbiodinium*. *Metabolites* **5**, 74-99.
Langlois, L. A. and Hoogenboom, M. O. (2014). Capacity for short-term physiological acclimation to light does not control the lower depth distributions of branching corals. *Mar. Ecol. Prog. Ser.* **508**, 149-162.
Lee, D.-K., Yoon, M. H., Kang, Y. P., Yu, J., Park, J. H., Lee, J. and Kwon, S. W. (2013). Comparison of primary and secondary metabolites for suitability to discriminate the origins of *Schisandra chinensis* by GC/MS and LC/MS. *Food Chem.* **141**, 3931-3937.
Lesser, M. P. and Shick, J. M. (1989). Effects of irradiance and ultraviolet radiation on photoadaptation in the zooxanthellae of *Aiptasia pallida*: Primary production, photoinhibition, and enzymic defenses against oxygen toxicity. *Mar. Biol.* **102**, 243-255.
Lesser, M. P., Marc, S., Michael, S., Michiko, O., Gates, R. D. and Andrea, G. (2010). Photoacclimatization by the coral *Montastraea cavernosa* in the mesophotic zone: Light, food, and genetics. *Ecology* **91**, 990-1003.
Liu, J., Liu, Y., Wang, Y., Abozeid, A., Zu, Y.-G. and Tang, Z.-H. (2017). The integration of GC–MS and LC–MS to assay the metabolomics profiling in *Panax ginseng* and *Panax quinquefolius* reveals a tissue- and species-specific connectivity of primary metabolites and ginsenosides accumulation. *J. Pharm. Biomed. Anal.* **135**, 176-185.
Lohr, K. E., McNab, A. A. C., Manfrino, C. and Patterson, J. T. (2017). Assessment of wild and restored staghorn coral *Acropora cervicornis* in three reef zones at Little Cayman, Cayman Islands. *Reg. Stud. Mar. Sci.* **9**, 1-8.
Matthews, J. L., Crowder, C. M., Oakley, C. A., Lutz, A., Roessner, U., Meyer, E., Grossman, A. R., Weis, V. M. and Davy, S. K. (2017). Optimal nutrient exchange

and immune responses operate in partner specificity in the cnidarian-dinoflagellate symbiosis. *Proc. Natl. Acad. Sci. USA* **114**, 13194-13199.
Meissner, S., Steinhauser, D. and Dittmann, E. (2015). Metabolomic analysis indicates a pivotal role of the hepatotoxin microcystin in high light adaptation of *Microcystis*. *Environ. Microbiol.* **17**, 1497-1509.
Muir, P. R., Wallace, C. C., Done, T. and Aguirre, J. D. (2015). Limited scope for latitudinal extension of reef corals. *Science* **348**, 1135-1138.
Muscatine, L. (1967). Glycerol excretion by symbiotic algae from corals and *Tridacna* and its control by the host. *Science* **156**, 516-519.
Muscatine, L. and Cernichiari, E. (1969). Assimilation of photosynthetic products of zooxanthellae by a reef coral. *Biol. Bull.* **137**, 506-523.
Muscatine, L., Falkowski, P. G., Porter, J. W. and Dubinsky, Z. (1984). Fate of photosynthetic fixed carbon in light- and shade-adapted colonies of the symbiotic coral *Stylophora pistillata*. *Proc. R. Soc. B Biol. Sci.* **222**, 181-202.
Nitschke, M. R., Gardner, S. G., Goyen, S., Fujise, L., Camp, E. F., Ralph, P. J. and Suggett, D. J. (2018). Utility of photochemical traits as diagnostics of thermal tolerance amongst Great Barrier Reef corals. *Front. Mar. Sci.* **5**, 45.
Obata, T. and Fernie, A. R. (2012). The use of metabolomics to dissect plant responses to abiotic stresses. *Cell. Mol. Life. Sci.* **69**, 3225-3243.
Porter, J. W., Muscatine, L., Dubinsky, Z. and Falkowski, P. G. (1984). Primary production and photoadaptation in light- and shade-adapted colonies of the symbiotic coral, *Stylophora pistillata*. *Proc. R. Soc. B Biol. Sci.* **222**, 161-180.
Quinn, R. A., Vermeij, M. J. A., Hartmann, A. C., Galtier d'Auriac, I., Benler, S., Haas, A., Quistad, S. D., Lim, Y. W., Little, M., Sandin, S. et al. (2016). Metabolomics of reef benthic interactions reveals a bioactive lipid involved in coral defence. *Proc. R. Soc. B Biol. Sci.* **283**, 20160469.
Ralph, P., Gademann, R., Larkum, A. and Kühl, M. (2002). Spatial heterogeneity in active chlorophyll fluorescence and PSII activity of coral tisses. *Mar. Biol.* **141**, 639-646.
Ross, A. M. (2014). Genet and reef position effects in out-planting of nursery-grown *Acropora cervicornis* (Scleractinia: Acroporidae) in Montego Bay, Jamaica. *Rev. Biol. Trop.* **62**, 95-106.
Roth, M. S. (2014). The engine of the reef: photobiology of the coral-algal symbiosis. *Front. Microbiol.* **5**, 1-22.
Schutter, M., van der Ven, R. M., Janse, M., Verreth, J. A. J., Wijffels, R. H. and Osinga, R. (2011). Light intensity, photoperiod duration, daily light flux and coral growth of *Galaxea fascicularis* in an aquarium setting: a matter of photons? *J. Mar. Biol. Assoc. UK* **92**, 703-712.
Shinzato, C., Shoguchi, E., Kawashima, T., Hamada, M., Hisata, K., Tanaka, M., Fujie, M., Fujiwara, M., Koyanagi, R., Ikuta, T. et al. (2011). Using the *Acropora digitifera* genome to understand coral responses to environmental change. *Nature* **476**, 320-323.
Sogin, E. M., Putnam, H. M., Anderson, P. E. and Gates, R. D. (2016). Metabolomic signatures of increases in temperature and ocean acidification from the reef-building coral, *Pocillopora damicornis*. *Metabolomics* **12**, 1-12.
Suescún-Bolívar, L. P., Iglesias-Prieto, R. and Thomé, P. E. (2012). Induction of glycerol synthesis and release in cultured *Symbiodinium*. *PLoS ONE* **7**, e47182.
Suggett, D. J., Moore, C. M., Hickman, A. E., Geider, R. J. (2009). Interpretation of fast repetition rate (FRR) fluorescence: signatures of community structure v physiological state. *Mar. Ecol. Prog. Ser.* **376**, 1-19.
Suggett, D. J., Hall-Spencer, J. M., Rodolfo-Metalpa, R., Boatman, T. G., Payton, R., Tye Pettay, D., Johnson, V. R., Warner, M. E. and Lawson, T. (2012). Sea anemones may thrive in a high CO_2 world. *Glob. Chang. Biol.* **18**, 3015-3025.
Titlyanov, E. A., Titlyanova, T. V., Yamazato, K. and van Woesik, R. (2001). Photo-acclimation dynamics of the coral *Stylophora pistillata* to low and extremely low light. *J. Exp. Mar. Bio. Ecol.* **263**, 211-225.
Torres, J. L., Armstrong, R. A., Corredor, J. E. and Gilbes, F. (2007). Physiological responses of *Acropora cervicornis* to increased solar irradiance. *Photochem. Photobiol.* **83**, 839-850.
Treignier, C., Tolosa, I., Grover, R., Reynaud, S. and Ferrier-Pagès, C. (2009). Carbon isotope composition of fatty acids and sterols in the scleractinian coral *Turbinaria reniformis*: Effect of light and feeding. *Limnol. Oceanogr.* **54**, 1933-1940.
Viant, M. R., Kurland, I. J., Jones, M. R. and Dunn, W. B. (2017). How close are we to complete annotation of metabolomes? *Curr. Opin. Chem. Biol.* **36**, 64-69.
Wangpraseurt, D., Larkum, A. W. D., Ralph, P. J. and Kühl, M. (2012). Light gradients and optical microniches in coral tissues. *Front. Microbio.* **3**, 316.
Warner, M. E. and Suggett, D. J. (2016). The photobiology of *Symbiodinium* spp.: Linking physiological diversity to the implications of stress and resilience. In *The Cnidaria, Past, Present and Future* (ed. S. Goffredo and Z. Dubinsky), pp. 489-509. Berlin: Springer Science and Business Media.
Warner, M. E., Lesser, M. P. and Ralph, P. J. (2010). Chlorophyll fluorescence in reef building corals. In *Chlorophyll a Fluorescence in Aquatic Sciences: Methods and Applications* (ed. D.J. Suggett), pp. 209-222. Berlin: Springer Science and Business Media.
Weckwerth, W. (2003). Metabolomics in systems biology. *Annu. Rev. Plant. Biol.* **54**, 669-689.
Winters, G., Beer, S., Zvi, B. B., Brickner, I. and Loya, Y. (2009). Spatial and temporal photoacclimation of *Stylophora pistillata*: Zooxanthella size, pigmentation, location and clade. *Mar. Ecol. Prog. Ser.* **384**, 107-119.
Wulff-Zottele, C., Gatzke, N., Kopka, J., Orellana, A., Hoefgen, R., Fisahn, J. and Hesse, H. (2010). Photosynthesis and metabolism interact during acclimation of *Arabidopsis thaliana* to high irradiance and sulphur depletion. *Plant Cell Environ.* **33**, 1974-1988.

Supplementary Figures

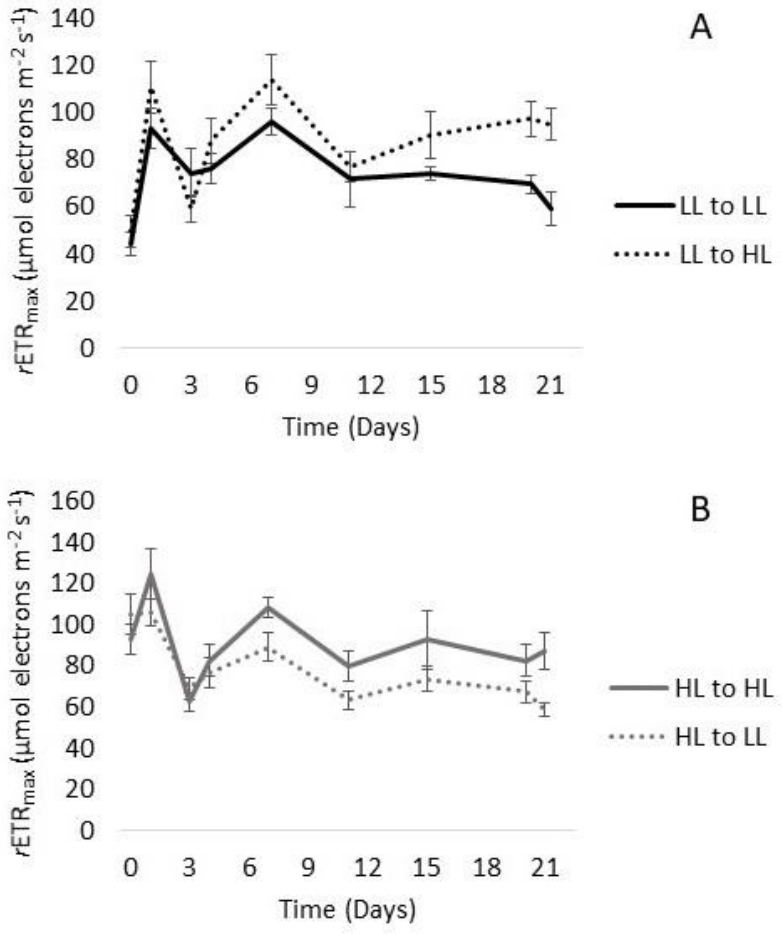

Figure S1 Maximum relative electron transport rate (*r*ETR^{MAX}) for (A) corals sourced from low light (LL, *n* = 24) and (B) corals sourced from high light (HL, *n* = 24) over time (means ± s.e.m.). A linear mixed model indicated that *r*ETR^{MAX} varied significantly based on source location only (HL vs. LL) at $t = 0$ ($p < 0.0001$). After one day of exposure to light treatments ($t = 1$), *r*ETR^{MAX} no longer varied based on source location, but did vary significantly based on treatment ($p = 0.01$). Light treatment also had a significant effect on *r*ETR^{MAX} (regardless of source location) at $t = 7$ ($p = 0.01$) and at the conclusion of the experiment ($t = 21$, $p < 0.01$), indicating photoacclimation over time.

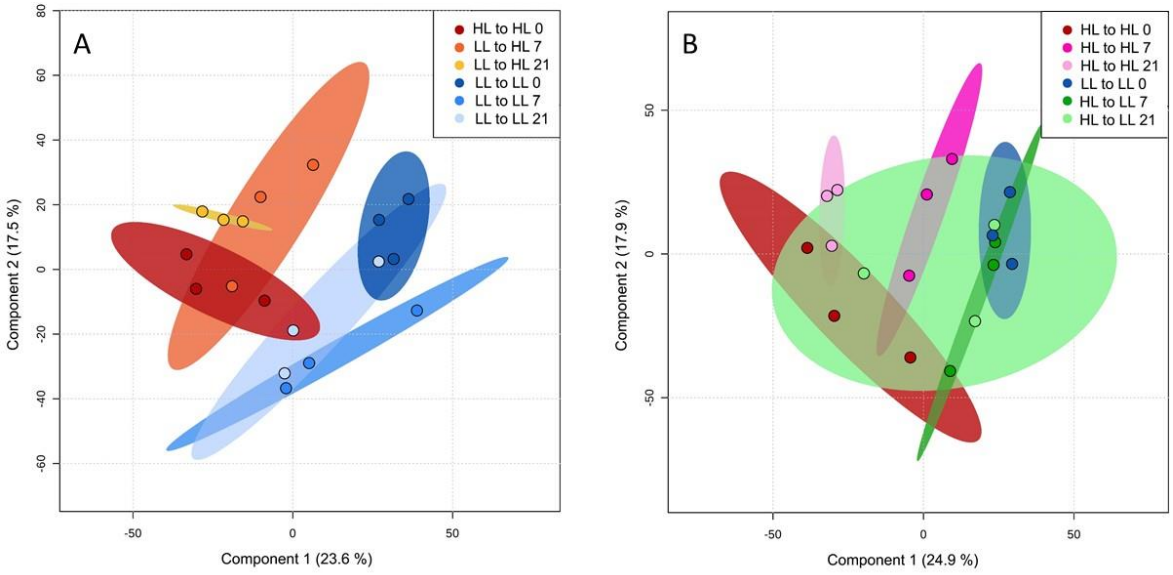

Figure S2 PCA results illustrating shifts in the metabolome over time based on GC-MS data for corals sourced from (A) LL and (B) HL. Each group consisted of n = 3 samples, and shading indicates 95% confidence intervals. Both panels illustrate distinct metabolomic profiles for HL to HL and LL to LL samples at t = 0. Panel A demonstrates that the metabolomes of LL to HL treated corals and LL to LL controls were distinct at t = 7 and t = 21. In contrast, panel B shows that the metabolomes of HL to LL treated corals and HL to HL controls are distinct at t = 7, but overlap at t = 21. Together, these results suggest metabolomic adjustment was more substantial for LL to HL treated corals compared to their HL to LL treated counterparts.

Journal of Experimental Biology • Supplementary information

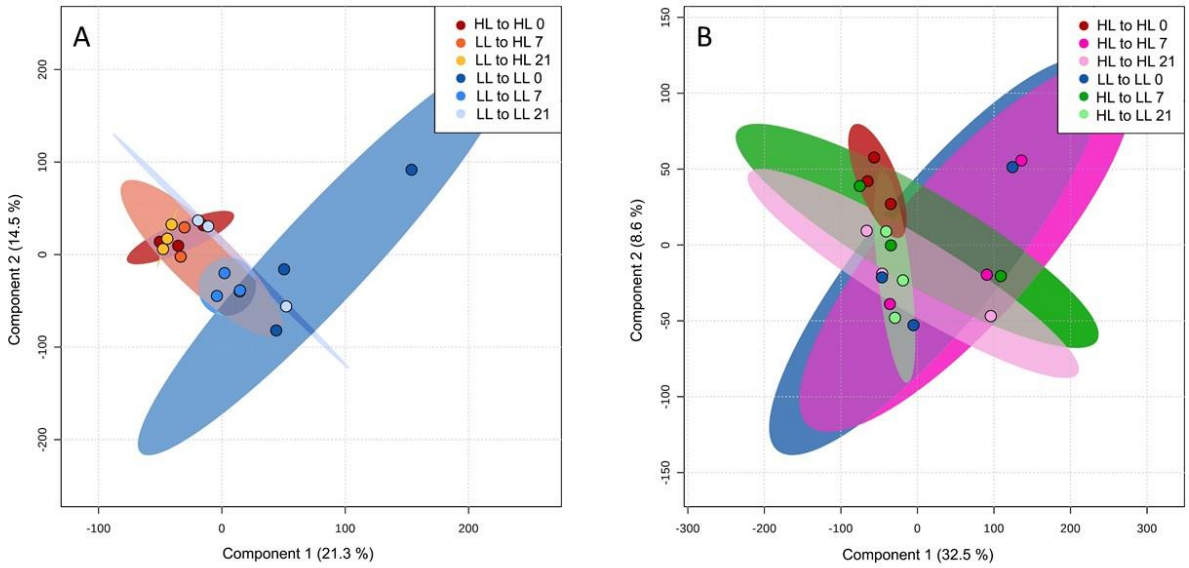

Figure S3 PCA results illustrating shifts in the metabolome over time based on LC-MS data for corals sourced from (A) LL and (B) HL. Each group consisted of n = 3 samples, and shading indicates 95% confidence intervals. Panel A illustrates distinct metabolomic profiles for HL to HL and LL to LL samples at t = 0. At t = 7, overlap was apparent between LL to HL treated colonies and LL controls, however separation was apparent between LL to HL treated corals and LL to LL controls at t = 21. Panel B shows substantial overlap between metabolomic profiles for HL to LL treated corals and HL to HL controls at every time point, as well as some overlap between HL to HL and LL to LL samples at t = 0. Together, these results suggest metabolomic adjustment was more substantial for LL to HL treated corals compared to their HL to LL treated counterparts.

Journal of Experimental Biology • Supplementary information

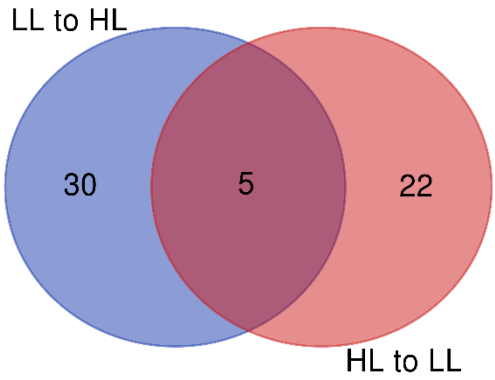

Figure S4 Venn diagram illustrating the number of features identified by LC-MS that changed over time in the LL to HL treatment group (*n* = 6) and the HL to LL treatment group (*n* = 6). Although no features resolved by LC-MS could be tentatively annotated, this diagram illustrates that very few of the same entities were altered by exposure to both high and low light.

Journal of Experimental Biology • Supplementary information